

# Estimation of sperm concentration and total motility from microscopic videos of human semen samples

Karan Dewan, Tathagato Rai Dastidar, Maroof Ahmad

SigTuple Technologies Pvt. Ltd, Bangalore, India

{karan, trd, maroof}@sigtuple.com

## Abstract

*We present a method for automated analysis of human semen quality using microscopic video sequences of live semen samples. The videos are captured through an automated microscope at 400× magnification. In each video frame, objects of interest are extracted using image processing techniques. A deep convolution neural network (CNN) is used to distinguish between sperms and non-sperm objects. The frame-wise count of sperm cells is used to estimate the concentration of sperms in unit volume of semen. In each video, individual sperm cells are tracked across the frames using a predictive approach which handles collisions and occlusions well. Based on their computed trajectories, sperms are classified into progressively motile, non-progressively motile and immotile types as per the WHO manual. In certain samples, due to various reasons, all visible objects drift in a certain direction. We present a method for identifying and compensating for the drift. Experimental results are presented on a set of more than 100 semen samples collected from a clinical laboratory. The results correlate well with existing accepted standard, SQA-V Gold for sperm concentration as well as motility parameters.*

## 1. Introduction

Semen quality assessment is performed for multiple reasons, ranging from analysis of male fertility to verifying results of a vasectomy procedure [1]. The assessment is performed manually by experts who view the live sperm sample under a microscope and obtain parameters such as sperm concentration per unit volume, morphological quality of the sperms, motility of the sperms, and the presence of non-sperm objects in the semen (e.g. white blood cells, crystals, spermatogonial cells, etc.). Based on all these criteria, which are measured along specific scales, the decision about the quality of semen is made. Due to rising fertility issues in men, the number of requests for the semen quality

analysis tests currently heavily overwhelms the number of available experts. Hence the motivation for this work.

To estimate the sperm concentration and motility, typically, an expert manually counts the number of sperms visible in a field of view of a microscope. A special counting chamber such as Makler chamber (or its variants) [14] can be used for more accurate analysis. The counted cells are further classified into different movement categories namely progressive (PR), non-progressive (NP) and immotile (IM) [16]. The manual process of counting is subjective and not very repeatable, frequently resulting in a large variance among counts reported by different experts.

Computer-aided-semen-analyzer systems (typically known as CASA machines), aim to partially automate this process, but are limited in their accuracy [19, 20]. Other systems, such as SQA-V Gold Semen Analyzer [3] which use a signal processing based technology (not based on microscopic images) are expensive, making them unsuitable for use in most laboratories in developing countries.

In this paper, we present a system – Aadi – which completely automates the semen analysis process. It consists of a digital microscope which automatically captures videos from a live semen sample at 400× magnification, using white light illumination. Most other automated analysis systems use a phase contrast microscope, which maps the phase shift in the light passing through transparent medium to brightness. [9]. It also does not require any specialized counting chambers. This makes the hardware component of Aadi extremely cost effective.

The primary advantages of Aadi over existing systems are the low cost of its hardware component [2], the accuracy of its sperm cell identification and tracking capabilities and its robustness to non-ideal processes during sample creation. In this paper we also show that the proposed technique is capable of successfully tracking a higher number of sperm cells in the field of view as compared to the results given in [18, 10, 11]. Unlike [4] we have evaluated our method on actual human semen samples.

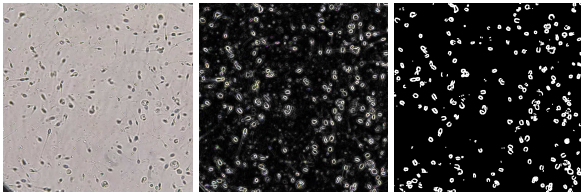
The contributions of this paper are:

- Resilient track classification to address the change in appearance of sperm cells as they move across a fluid medium at varying depths.
- Detection and estimation of drift from semen samples.

The paper is organized as follows: Section 2 lays out details about input and generation of detection responses for tracking, Section 3 explains the method used for generation of trajectories, section 4 explains the trajectory classification using CNN and 5 details out the method for estimation of total sperm concentration and total sperm motility.

## 2. Generation of object proposals

Input to our pipeline is a set of microscopic videos at from a microscope camera. In order to generate the object proposals from the input, we employ [5] a blob detection technique to identify candidate sperm cell objects. These candidates are then tracked across the video frames to generate trajectories. To detect blobs we start off by converting each frame  $I$  to a gray-scale image  $I_g$  followed by a Gaussian blur based de-noising. A Sobel based edge detection [8] is then applied on the de-noised image to extract an edge image,  $I_s$ , which is then thresholded. An empirical threshold of 64, selected based on trial-and-error, is used for this process. Morphological image opening is then applied on  $I_s$  to remove noise, resulting in a binary image  $I_m$ . Connected components [8] are identified in  $I_m$ , and those connected components whose area lie between the biological limits of the size of a sperm cell, are retained as object proposals for further processing. Refer figure 1



(a) Input Image (b) Sobel image (c) Extracted blobs

Figure 1: Process for generation of object proposals. The original input image is shown in 1a. 1b shows the output of the sobel edge detection step and 1c shows the extracted blobs as the object proposals.

## 3. Generation of sperm trajectories

We track the object proposals through the video sequence to generate candidate trajectories for identification of sperm movement. Trajectories are created using into the following three step process.

1. Generation of tracklets, track fragments which are chained to form a trajectory.

2. Association of tracklets
3. Compensation for *drift motion*

### 3.1. Generation of tracklets

One of the challenging aspect of any tracking problem is to form a correct association between a new detection in the current frame with one of the existing tracks. The problem of tracking sperm cells is very unlike normal video tracking problems reported in the literature, e.g. [13, 12]. The movement pattern of sperms is very complex, with sudden changes in direction [7]. Sperms also frequently move from the surface of the seminal liquid to a lower layer, which drastically changes their appearance. Thus, it is difficult to create a motion model for sperm cells. We combine the detection responses from the extraction phase – the object proposals – for neighboring frames into tracklets by using an association cost between the responses across these frames.

A tracklet in our case can be denoted as

$$T_i = [d_i^{t_n}] \quad n = 1 \dots N_i \quad (1)$$

$N_i$  is the number of frames in the tracklet  $T_i$ ,  $d_i^{t_n} = (x_n, y_n)$ , represents a detection response for the  $i^{\text{th}}$  tracklet at time  $t_n$ . The association of detections for a single tracklet would then define the motion of a single sperm cell in the video sequence from  $t_1 \rightarrow t_{N_i}$ . Detailed process for generating the motion trajectories is outlined below.

For each detection in  $\{d_1^{t_s}, d_2^{t_s}, \dots, d_K^{t_s}\}$ , in the frame with a time-stamp  $t_s$  we either:

- Associate it with an existing track by solving a generalized assignment problem based on some association cost, or,
- Initialize a new track for that detection, if it cannot be associated with an existing track.

The cost of assignment for the  $i^{\text{th}}$  detection at time  $t_s$  to the  $j^{\text{th}}$  existing track ( $T_j$ ) is calculated as  $C_{ij}^{t_s}$ .

$$C_{ij}^{t_s} = \begin{cases} \|d_i^{t_s} - P_j^{t_s}\|_2 & \text{if } \|d_i^{t_s} - P_j^{t_s}\|_2 \leq 15\mu m \\ \infty & \text{otherwise} \end{cases} \quad (2)$$

Here,  $P_j^{t_s}$  refers to the prediction from the track  $T_j$  at time  $t_s$  and is calculated as

$$P_j^{t_s} = \begin{bmatrix} c_x & v_x \\ c_y & v_y \end{bmatrix} * \begin{bmatrix} 1 \\ t_s \end{bmatrix} \quad (3)$$

$v_x, c_x$  and  $v_y, c_y$  are calculated by minimizing a residual from the following overdetermined motion model,

$$\begin{bmatrix} t_1 \\ t_2 \\ \vdots \\ t_{s-1} \end{bmatrix} \begin{bmatrix} v_x \\ v_y \end{bmatrix}^T + \mathbf{1} \begin{bmatrix} c_x \\ c_y \end{bmatrix}^T = \begin{bmatrix} x_1 & y_1 \\ x_2 & y_2 \\ \vdots & \vdots \\ x_{s-1} & y_{s-1} \end{bmatrix} \quad (4)$$

Here,  $(x_k, y_k)$ ,  $k = 1, \dots, s - 1$  are previous detection responses assigned to a particular tracklet up to a time  $t_{s-1}$ .

In order to correctly associate a new detection to one of the existing tracklets, we model the problem as a generalized version of linear assignment sum as follows,

$$\min \sum_{i=1}^m \sum_{j=1}^K C_{ij} x_{ij} \quad (5)$$

such that.

$$\sum_{i=1}^m x_{ij} = 1 \quad j = 1, \dots, n \quad (6)$$

where  $X = [x_{ij}]$  is a boolean matrix where a true value represents an association between a tracklet and a new detection. Here  $m$  is the number of active tracklets and  $K$  is the number of new detections in frame with time stamp  $t_s$ . We compute the cost matrix  $C = [C_{ij}]$  with each element representing a cost of assignment between the  $i^{\text{th}}$  track and the  $j^{\text{th}}$  detection in the current frame.

This problem can be solved using the Hungarian algorithm [15] to generate matches between the tracklets and the new candidate detections. However, solving the above problem using the Hungarian algorithm becomes slower with increasing number of tracklets (or detections). The linear sum assignment problem is also known as minimum weight matching in bipartite graphs. The cost-of-assignment matrix  $C$  is likely to have a lot of infinite cost elements as there will be obvious non matches due to spatial constraints (detections too far apart from each other will have infinite cost of association). Thus, we will have many small connected components in  $C$  when it is viewed as a bipartite graph. These individual connected components can then be solved independently for the minimum weight matching to compute the complete solution. The bipartite graph is also sparse allowing for the use of efficient storage and computation methods for solving. We use a KD-Tree data-structure [6] for efficient cost calculation using the equation 2.

For all valid assignments we update the tracklets with the assigned detection and time stamp. We also start new tracklets for all the unassigned detections. To keep track of assignments and invalidate inactive tracklets over time we maintain a ‘‘continuous invisible count’’ for all trajectories. This denotes the number of frames for which there were

no assigned detections to the tracklet. The count gets incremented for a tracklet if it doesn’t see any association in the current frame. This count is reset for the track when it gets associated with a detection. This allows us to discard tracks from active pool if they are not associated with a new detection for a long time. Refer Figure 2.

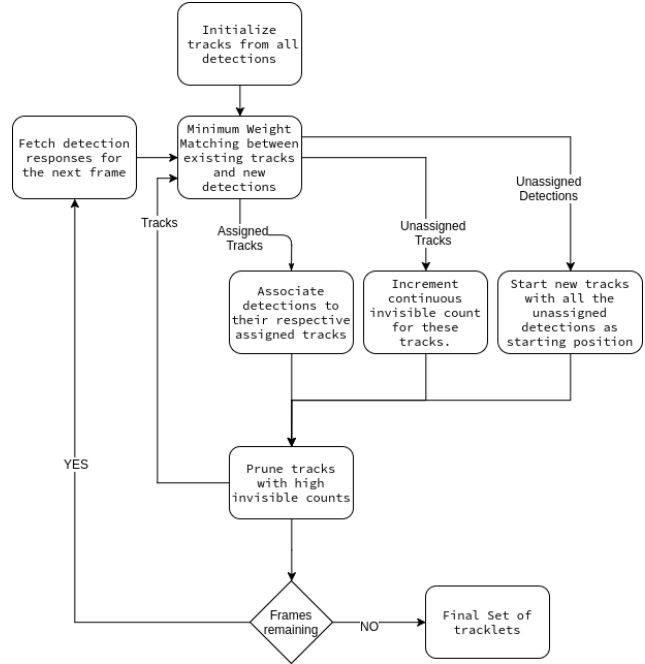


Figure 2: Generation of sperm tracklets.

### 3.2. Associate tracklets belonging to same trajectory

Sperm trajectories may be *broken* in between if there are no detections for a few frames. This can cause a real trajectory to be split into two or more tracklets. To counter this, tracklets obtained using the above algorithm are further associated with other tracklets if they are deemed to belong to the same trajectory. A set of associated tracklets are then joined to form a single tracklet which will represent a complete sperm trajectory. In order to achieve this, we create a graph with each node representing a tracklet from the tracking stage. A directed edge in this graph represents the likelihood of the two tracklets belong to the same trajectory, with the *from* node as the precursor and the *to* node being the descendant. Let  $T_i$  and  $T_j$  be tracklets from the tracking stage corresponding to the graph nodes  $i$  and  $j$  respectively. Also we have  $t_i^s$  and  $t_i^e$ , the start and end time for  $T_i$ . If  $T_i$  is a precursor of  $T_j$ , then the required condition for them to be associated is  $t_i^e < t_j^s$  (or  $t_j^e < t_i^s$  if  $T_j$  is a precursor of  $T_i$ ). The weight of the directed edge between the nodes  $i$  and  $j$

would then be calculated as,

$$W_{i \rightarrow j} = \begin{cases} \|d_i^{t^e} - d_j^{t^s}\|_2 & t_i^e < t_j^s \wedge t_j^s - t_i^e < 100\text{ms} \\ \infty & \text{otherwise} \end{cases} \quad (7)$$

where,  $d_i^{t^e}$  and  $d_j^{t^s}$  are the detection responses of the tracklet  $i$  at end time and  $j$  at start time respectively. An edge-weight of  $\infty$  represent no edge or a disconnection. We can view the above tracklet-level association graph as a bipartite matching problem as shown in the figure 3. We can solve the above bipartite matching problem using the method provided in Section 3.1. After solving the assignment problem on the bipartite representation we transform it back into the the directed tracklet-level association graph. We find the individual connected components of the association graph to obtain a chain of associated tracklets, which are then joined to form a final trajectory.

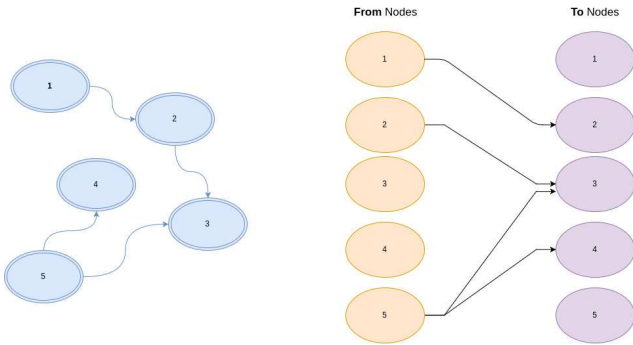


Figure 3: Viewing the tracklet association as a maximum weight bipartite matching problem.

### 3.3. Compensation for drift motion

Drift is characterized a homogeneous movement of all sperm cells and other particles in a dominant direction. Our observation is that in certain samples, all visible objects in the fluid drift in a certain direction. Presence of a continuous drift in fluid will cause an erroneous report to be generated as sperm motility will be overestimated. There are various well known causes for drift. Some of the common causes are excess sample volume, bending of the microscope stage used for imaging, i.e., if the platform on which the sample is kept is not perfectly horizontal, etc. Presence of such drift in the sample will cause all the non-sperm objects and immotile sperms (which have no flagellar beat) to move at a constant speed in the direction of the drift. Since the sample preparation process is manual, such errors cannot be entirely ruled out under normal usage, and thus we need to detect and compensate for drift motion.

We present a method to estimate a drift velocity entirely from the particle/sperm trajectories in the sample. In a normal sample with no drift, sperm cell movements are nearly

random and in all directions. In order to detect the presence of a drift motion in a sample we employ a velocity correlation method where we create a correlation matrix with the  $x$  and  $y$  components for the straight-line velocities (VSL) of the sperm movement, we define

$$\mathbf{X} = \begin{bmatrix} v_x^1 & v_y^1 \\ v_x^2 & v_y^2 \\ \vdots & \vdots \\ v_x^n & v_y^n \end{bmatrix} \quad (8)$$

$$\Sigma = \mathbf{X}^\top \mathbf{X} \quad (9)$$

Here,  $n$  is the total number of tracklets.

The Eigenvalue decomposition of the above  $\Sigma$  matrix yields 2 eigenvalues. We arrange them in descending order ( $\lambda_1, \lambda_2$  with  $\lambda_1 > \lambda_2$ ). For a sample with no significant drift component the ratio  $\lambda_1/\lambda_2$  is small (near to 1). For samples with a drift component present this ratio exhibits a large value. However, the corresponding eigenvector may or may not correspond exactly to the drift direction since there will be effects of other sperm movements.

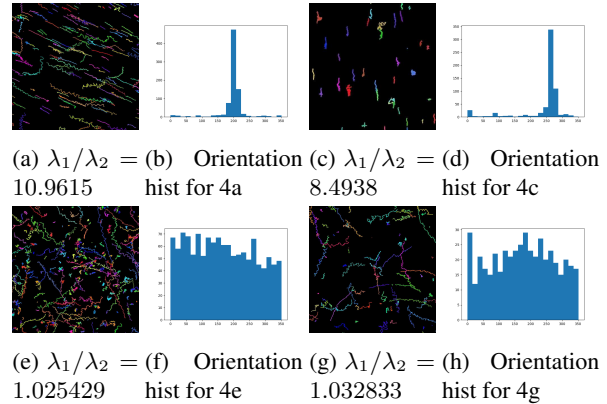


Figure 4: Estimation of drift direction. Where  $\lambda_1$  and  $\lambda_2$  are the Eigen values of the correlation matrix of straight line velocities with  $\lambda_1 > \lambda_2$ . Figures 4a and 4c show samples with higher amount drift while 4e and 4g show samples with no drift

To deduce the magnitude of this detected drift motion we form a histogram for the orientations of all trajectories into  $N$  orientation bins. In case of drift, one of these bins will have significantly more objects than others (refer Figure 4). We calculate a median velocity of drift motion ( $v_{\text{drift}}$ ) by finding the median of all velocities present in the dominant orientation bin. Next, the drift velocity is subtracted from the velocity of every tracklet (vector subtraction), before computing the linear velocity and other motility parameters.

## 4. Classification of trajectories into sperm and non-sperm categories

Several semen samples may also contain certain non-sperm objects which may be indicative of testicular damage (immature germ cells), pathology of the efferent ducts (ciliary tufts) or inflammation of the accessory glands (leukocytes). Since these objects are also captured by our method we need to classify the corresponding trajectories generated by such non-sperm entities, before the estimation for the total sperm concentration and motility is performed.

As a result of this step we calculate the ratio of sperm trajectory presents,  $T_{\text{sperm}}$ , as,

$$T_{\text{sperm}} = \frac{\text{Number of sperm-trajectories}}{\text{Total number of trajectories}} \quad (10)$$

### 4.1. Method

As indicated above tracking phase yields multiple trajectories, for motile cells, immotile cells, and other non-sperm objects, refer Figure 6b While a sample of depth  $20\mu m$ , which is the recommended value as per [16], allows for free sperm movement, it also causes the movement of sperm cells across multiple depths of the sample under observation. This particular behavior leads to varying appearance of these cells as they move across the focal plane. Refer Figure 6a. In order to address the above mentioned issues we randomly sample  $n$  detections from each trajectory and then pass them through a Convolution Neural network (CNN). The CNN classifies each random patch generated from the trajectory into a sperm or a non-sperm entity, figure 5. The majority of the predicted classes (either sperm or non-sperm) for the  $n$  sampled detections of a trajectory is taken as the class of that trajectory. This method builds resilience for the drastic appearance change of sperm cells when they move across layers. It is also more computationally efficient than the naive method of classifying every object proposal at every frame of the video. This allows us to eliminate certain trajectories related to non-sperm immotile objects.

### 4.2. Network architecture and training

The architecture of CNN used for classification of sperm vs non-sperm entities consists of a 5 layer network with 3 convolution layers consisting of 16, 32 and  $64 \times 3$  filters respectively. These are followed 2 fully connected layers comprising of 256 neurons each and a 2 node soft max layer for the classification output. We used a learning rate of .001 with Adam's optimizer for training the model.

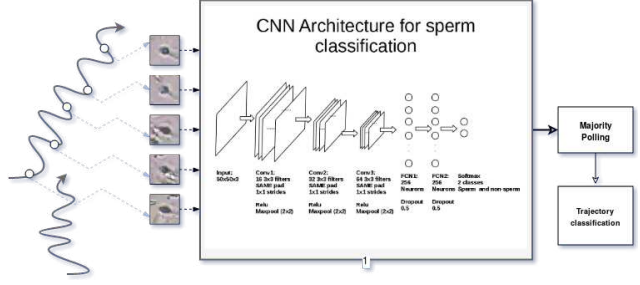


Figure 5: Trajectory classification is done by randomly sampling a few detections from the trajectory followed by their classification using a CNN and majority pooling.



(a) Sperm cells. (b) Non-sperm entities.

Figure 6: Sample images from training set

## 5. Estimation of Screening Parameters

### 5.1. Velocity computation

After association of tracklets we calculate various metrics to characterize the spermatozoa movement (Refer Figure. 7). These include:

1. Curvilinear velocity (VCL,  $\mu m/s$ ), which is the time-averaged velocity of a sperm head along its actual curvilinear path, as perceived in two dimensions under the microscope. This is a measure of cell vigour.
2. Straight-line velocity (VSL,  $\mu m/s$ ), time-averaged velocity of a sperm head along the straight line between its first detected position and its last.

$$VCL = d_{\text{actual}}/\text{duration}$$

$$VSL = d_{\text{displacement}}/\text{duration}$$

3. Average path velocity (VAP,  $\mu m/s$ ). Time averaged velocity of sperm head along about its average path. This path is calculated by smoothing out the trajectory using the Kalman Filter algorithm .
4. Linearity (LIN). The linearity of a curvilinear path, calculated as  $VSL/VCL$ .

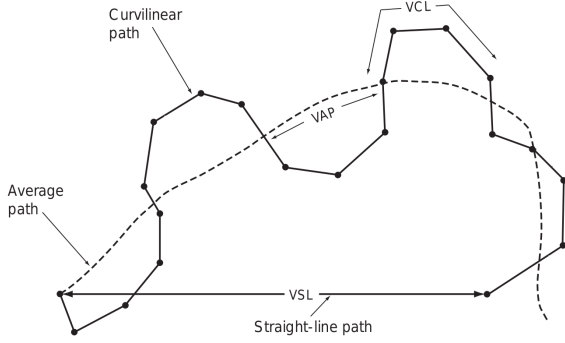


Figure 7: Standard terminology for variables measured by our system. [16]

## 5.2. Estimation of Total sperm concentration

We infer the total sperm count for a sample by calculating the average foreground area for the FOV using the method described in the section for generation of object proposals (Refer Section 2). We then incorporate the fraction of trajectories classified as sperms as a decay factor for the average area and use the linear relationship as shown below to estimate the final concentration in **Millions/mL**.

$$C = \alpha * (A_{fg} * T_{sperm}) + \beta$$

where,  $C$  is the concentration calculated,  $A_{fg}$  is the average foreground area calculated as described above and  $T_{sperm}$  represents the fraction of trajectories which are classified as sperm trajectories as described in Section 4.  $\alpha$  and  $\beta$  represent the coefficients to map the average area value to concentration to the unit **Millions/mL**.

## 5.3. Estimation of Motility parameters

The motility parameters are assessed using the measurement of the straight-line velocities of the trajectories obtained.

Since we also assume a homogeneous drift motion model for the fluid, the calculated drift velocity (in  $v_{drift}$ ) is subtracted from all the existing straight-line velocities vector  $V_{vsl}$ . These drift compensated velocities  $V_{vsl}^{drift}$  are then further used for estimation of motility parameters:

$$V_{vsl}^{drift} = V_{vsl} - v_{drift}$$

In order to obtain the total immotile concentration and account for any tiny amount of remaining drift motion we use a threshold of  $1\mu m/s$ . Trajectories having velocities below this are regarded as immotile sperm cells. The immotility(or motility) is calculated by calculating the immotile count(motile count) as percentage of the total number of trajectories.

## 6. Experiments and Results

**Experimental setup:** The input to the system is a set of videos, captured by our digital microscope [2], at  $400\times$  magnification with a digital resolution of  $3200 \times 2400$ . The slide is prepared by placing a volume of  $10\mu L$  semen sample at the center of the slide followed by placement of a  $22 \times 22mm$  transparent plastic cover slip on it. The weight of the cover slip causes the liquid to spread out, and gives a sample depth of approx.  $20\mu L$  which is consistent with the recommendation in WHO'99 [16]. The slide is placed in the automated microscope for video capture, about 90 frames at 30fps, of a number of different fields of views (FOVs). The details of the automated capture algorithm are beyond the scope of this paper.

**Dataset:** The training data for the CNN introduced in 4 consists of about 3800 images of size  $50 \times 50$  captured at a resolution of 4 pixels per microns. These images are annotated by a pathologist into one of the two categories of sperm vs. non-sperm cell.

We evaluated the following parameters reported by Aadi.

1. Total Sperm Concentration
2. Total Motility Percentage
3. Tracking performance

The significance of performance of our solution is measured with respect to an automated, signal processing based, semen analyzer SQA-V Gold augmented with manual counts for missing and anomalous readings.

### 6.1. Total Sperm Concentration

We performed a Passing-Bablok regression [17] analysis for the total concentration estimates from Aadi and SQA-V Gold, a signal processing based semen analyzer solution. Here B1 is the slope of the linear fit obtained by the Passing-Bablok regression and B0 is the bias value obtained.

In comparison of our method with SQA-V Gold we obtain a B1 value of 1.665 with 95 % confidence interval of (1.5 to 1.8) and B0 value of 1.91 and confidence interval of (-12.6 to -0.57).

### 6.2. Total Motility Percentage

Similar to section 6.1 we again perform Passing-Bablok regression. The following points show the results obtained as a part of the the Passing-Bablok regression analysis. In Comparison of our method with SQA-V Gold we obtain a B1 value of 1.41 with 95 % confidence interval of (1.28 to 1.69) and B0 value of -16.12 and confidence interval of (-24.4 to -9.4).

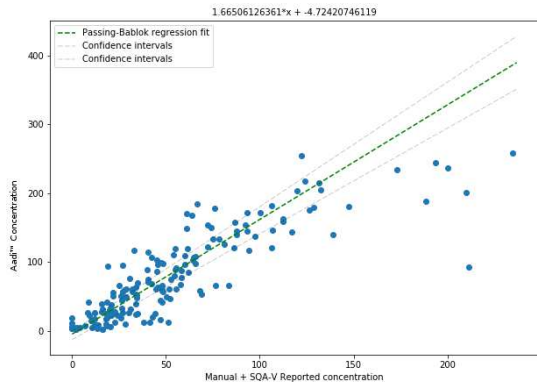


Figure 8: Reported concentration by SQA-V Gold vs. Estimated Concentration (C)

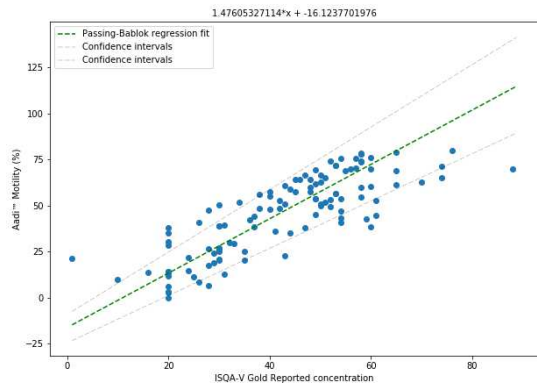


Figure 9: Report Total Motility percentage (by SQA-V Gold) vs. Estimated Motility percentage.

Parameter	Pearson Coefficient
Total Concentration	0.86
Total Motility %	0.818

Table 1: Pearson Correlation of Semen quality indicators with that reported by SQA-V Gold Semen analyzer.

### 6.3. Tracking Performance

We evaluated tracking performance on a subset of sample videos used for the above experiments. Tracked sperm cells in those videos are visualized in Figure 10.

To determine the miss-rate we overlaid the tracks and a square grid over a set of 79 videos. A set of individuals were then asked to count the number of sperm cells missed for any 10 random squares for each video sample and the

number was then extrapolated to get an estimate of miss for the complete FOV. The mean miss percentage was 7.44%. Also 75 percentile of the video samples had miss rate below 10% and around 95 percentile had a miss rate of around 22%.

## 7. Conclusion

In this paper, we present a resilient tracking mechanism for sperms in a multi-layered wet-mount slide. We address the problem of the changing appearance of sperm cells using a generalized version of linear assignment sum followed by a deep CNN for classification. In addition, we also solve for the drift associated with wet mount cells by estimating the overall drift velocity vector using the trajectories of the sperm candidates. Our method also deals with occlusions occurring due to the z-axis movement of sperm cells in the fluid.

The sperm trajectories are further used to calculate clinical parameters associated with fertility and viability of the sample. As presented in Sec. 6, we provide comparisons with the current accepted standard, SQA-V Gold, an automated semen analyzer. Our method is comparable with the SQA-V Gold on both the motility and the concentration parameters. In the future, we would like to augment this solution by adding morphology analysis of sperm cells to identify vital sperm cells.

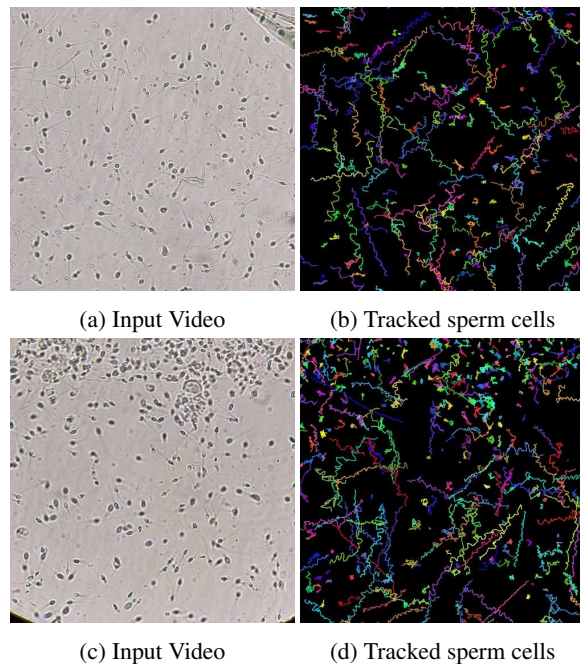


Figure 10: Visualization of tracked sperm cells.

## References

- [1] Healthline. <http://www.healthline.com>.
- [2] Sigtuple. <https://sigtuple.com/>.
- [3] Sqa-vision — the ultimate automated semen analysis solution for hospitals, reproductive centers, free standing labs, and cryobanks. <http://mes-global.com/analyzers>.
- [4] A. Arasteh and B. V. Vahdat. Evaluation of multi-target human sperm tracking algorithms in synthesized dataset. *International Journal of Monitoring and Surveillance Technologies Research (IJMSTR)*, 4(2):16–29, 2016.
- [5] I. N. Bankman and S. Morcovescu. Handbook of medical imaging. processing and analysis. *Medical Physics*, 29(1):107–107, 2002.
- [6] J. L. Bentley. Multidimensional binary search trees used for associative searching. *Communications of the ACM*, 18(9):509–517, 1975.
- [7] B. Friedrich, I. Riedel-Kruse, J. Howard, and F. Jülicher. High-precision tracking of sperm swimming fine structure provides strong test of resistive force theory. *Journal of Experimental Biology*, 213(8):1226–1234, 2010.
- [8] R. C. Gonzalez, R. E. Woods, et al. Digital image processing, 2002.
- [9] R. Green, E. Gillies, R. Cannon, and A. Pacey. Analysis of cell morphology and motility, Dec. 27 2007. US Patent App. 10/589,882.
- [10] Y. Imani, N. Teyfour, M. R. Ahmadzadeh, and M. Golabakhsh. A new method for multiple sperm cells tracking. *Journal of medical signals and sensors*, 4(1):35, 2014.
- [11] G. Jati, A. A. Gunawan, S. W. Lestari, W. Jatmiko, and M. Hilman. Multi-sperm tracking using hungarian kalman filter on low frame rate video. In *Advanced Computer Science and Information Systems (ICACSIS), 2016 International Conference on*, pages 530–535. IEEE, 2016.
- [12] W.-L. Lu, J.-A. Ting, J. J. Little, and K. P. Murphy. Learning to track and identify players from broadcast sports videos. *IEEE transactions on pattern analysis and machine intelligence*, 35(7):1704–1716, 2013.
- [13] W.-L. Lu, J.-A. Ting, K. P. Murphy, and J. J. Little. Identifying players in broadcast sports videos using conditional random fields. In *Computer Vision and Pattern Recognition (CVPR), 2011 IEEE Conference on*, pages 3249–3256. IEEE, 2011.
- [14] A. Makler. A new chamber for rapid sperm count and motility estimation. *Fertility and sterility*, 30(3):313–318, 1978.
- [15] J. Munkres. Algorithms for the assignment and transportation problems. *Journal of the society for industrial and applied mathematics*, 5(1):32–38, 1957.
- [16] W. H. Organization et al. Who laboratory manual for the examination and processing of human semen. 2010.
- [17] H. Passing and W. Bablok. A new biometrical procedure for testing the equality of measurements from two different analytical methods. application of linear regression procedures for method comparison studies in clinical chemistry, part i. *Clinical Chemistry and Laboratory Medicine*, 21(11):709–720, 1983.
- [18] L. Sørensen, J. Østergaard, P. Johansen, and M. de Bruijne. Multi-object tracking of human spermatozoa. In *Medical Imaging 2008: Image Processing*, volume 6914, page 69142C. International Society for Optics and Photonics, 2008.
- [19] I. Susrama, K. Purnama, and M. Purnomo. Automated analysis of human sperm number and concentration (oligospermia) using otsu threshold method and labelling. In *IOP Conference Series: Materials Science and Engineering*, volume 105, page 012038. IOP Publishing, 2016.
- [20] M. J. Tomlinson, K. Pooley, T. Simpson, T. Newton, J. Hopkisson, K. Jayaprakasan, R. Jayaprakasan, A. Naeem, and T. Pridmore. Validation of a novel computer-assisted sperm analysis (casa) system using multitarget-tracking algorithms. *Fertility and sterility*, 93(6):1911–1920, 2010.